Electronic Supplementary Material (ESI) for Journal of Materials Chemistry A.

Supplementary Information for

Asymmetric PdPtCu Mesoporous Hemispheres on Nitrogen-Functionalized Graphene for Methanol Oxidation Electrocatalysis

Lizhi Sun,[†] Hao Lv,[†] Dongdong Xu, and Ben Liu*

Jiangsu Key Laboratory of New Power Batteries, Jiangsu Collaborative Innovation Center of Biomedical Functional Materials, School of Chemistry and Materials Science, Nanjing Normal University, Nanjing 210023, China

[†]L. Sun and H. Lv contributed equally to this work.

*Email: ben.liu@njnu.edu.cn

Table of Contents

1. Chemicals and Materials

Palladium(II) chloride ($PdCl_2$), chloroplatinic acid (H_2PtCl_6), copper nitrate ($Cu(NO_3)_2$), disoctyl dimethyl ammonium chloride, dimethyl distearylammonium chloride, dihexadecyldimethylammonium chloride, dioctadecyldimethylammonium chloride (DODAC), and *L*-ascorbic acid (AA) were obtained from Alfa Aesar. Commercial Pd/C (30 wt %) and Nafion solution (5 wt % in alcohol and H_2O) were purchased from Sigma Aldrich. Nitrogen-functionalized graphene (N-G with N content of 3.0-5.0 wt %) and graphene oxide (GO) were purchased from Nanjing XFNANO Materials Tech Co. Ltd. Hydrochloric acid (HCl), ethanol, sodium hydroxide (NaOH), and potassium hydroxide (KOH) were obtained from Sinopharm Chemical Reagent Co. Ltd. (Shanghai). To prepare 10 mM (mmol/L) H_2PdCl_4 solution, 0.355 g of $PdCl_2$ was dissolved with 20 mL of 0.2 M HCl solution in a 200 mL volumetric flask and further diluted to 200 mL by deionized H_2O. All the reagents are of analytical reagent grade and used without further purification. Deionized H_2O with the resistivity of 18.25 mΩ was used in all experiments.

2. Synthesis of Asymmetric PdPtCu MHSs@N-G and their counterparts

Asymmetric PdPtCu mesoporous hemispheres (MHSs) on N-G (PdPtCu MHS@N-G) was synthesized by a solution-phase route with DODAC as a surfactant template, H_2PdCl_4, H_2PtCl_6 and $Cu(NO_3)_2$ as metal precursors, AA as a reducing agent, and N-G as a functionalized support. In a typical synthesis, 3.0 mg of DODAC was first dissolved in 10 mL of co-solvents with ethanol/H_2O with a volume ratio of 2 : 8, followed by the addition of 0.1 mL of 0.1 M HCl. Then, 0.48 mL of 10 mM H_2PdCl_4, 0.24 mL of 10 mM H_2PtCl_6, 0.24 mL of 10 mM $Cu(NO_3)_2$, and 0.4 mL of 1.0 mg mL^{-1} N-G were successively added, and further incubated at 25°C for 30 min. Subsequently, 1.0 mL of freshly prepared 0.3 M AA was injected with gentle shaking. The color of the solution was immediately changed from yellow to black, implying the formation of trimetallic PdPtCu alloys. After incubating undisturbed for 60 min, asymmetric PdPtCu MHS@N-G was obtained by centrifuged and washed three times with ethanol/H_2O to remove the surfactant on/within the MHSs. Similarly, metallic Pd MHS@N-G and bimetallic PdPt MHS@N-G were synthesized using a similar procedure, but different metal precursors. In contrast, PdPtCu MSs were synthesized with the same reactants except in the absence of N-G. Besides, synthetic conditions were tuned to optimize the structure of asymmetric PdPtCu MHS@N-G.

3. The preparation of nanocatalysts ink

Before electrocatalysis, the nanocatalysts and work electrode [glassy carbon electrode (GCE, 0.07065 cm^2)] were thoroughly cleaned with H_2O/ethanol. The ink of the catalyst was prepared as followed: 1.0 mg of nanocatalyst was mixed into 0.75 mL of ethanol and 0.25 mL of H_2O, and sonicated for 30 min. Then, 50 μL of Nafion solution

(5 wt % in alcohol and H_2O) was injected and further sonicated for 30 min. Lastly, 3.0 µL of the prepared ink solution was directly casted on the GCE electrode and dried at 40 °C before the test.

4. Electrochemical oxidation of organic fuels

Electrocatalytic studies were carried out on a CHI 660E electrochemical analyzer at 25 °C. All electrochemical tests used a three-electrode system in which a GCE was used as working electrode, a carbon rod as counter electrode, and a silver/silver chloride electrode as reference electrode. The potentials used in this work were reported with respect to the saturated calomel electrode (SCE). The cyclic voltammogram (CV) was continuously scanned until a stable curve was obtained for further removal of the surfactant in N_2-saturated 1.0 M KOH. The mass activity of the nanocatalyst for the electrooxidation of methanol was collected by scanning CV in 1.0 M KOH and 1.0 M methanol at a scan rate of 50 mV s^{-1}. In contrast, we evaluated electrooxidation of ethanol in 1.0 M KOH and 1.0 M ethanol, electrooxidation of glycerol in 1.0 M KOH and 0.1 M glycerol, electrooxidation of glucose in 0.1 M NaOH and 0.01 M glucose, and electrooxidation of formic acid in 1.0 M HCOOH and 0.5 M H_2SO_4.

E_a was calculated based on Arrhenius equation as below:

$$I = \mathrm{A}^{-Ea/\mathrm{RT}}$$

where I is the current at a specific potential, R is the gas constant, T is the temperature in K, and E_a is the apparent activation energy.

5. Characterizations

Transmission electron microscopy (TEM) observations were performed at 200 kV using a JEOL JEM-2100 microscope. High-angle circular dark-field scanning TEM (HAADF-STEM) was performed on FEI Talos F200X device with an acceleration voltage of 200 kV, which is also equipped with an EDS detector for element mapping analysis. TEM and STEM samples were prepared by casting a sample suspension onto a carbon coated nickel grid (300 mesh). Wide-angle X-ray diffraction (XRD) patterns were obtained on powder samples using a D/max 2500 VL/PC diffractometer (Japan) equipped with graphite-monochromatized Cu Kα radiation. X-ray photoelectron spectroscopy (XPS) was performed using a scanning x-ray probe of Al Kα radiation (thermal ESCALAB 250 Xi). The binding energy of the C 1s peak (284.8 eV) is used as a criterion for calibrating the binding energy of other elements.

6. Figures and Table

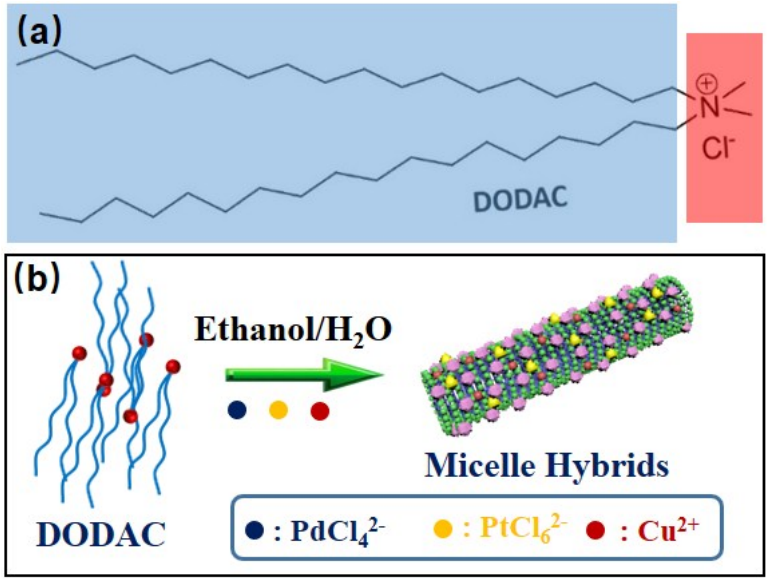

Figure S1. (a) Chemical structure of DODAC. (b) A scheme illustrating self-assembled cylindrical phase of DODAC and metal precursors.

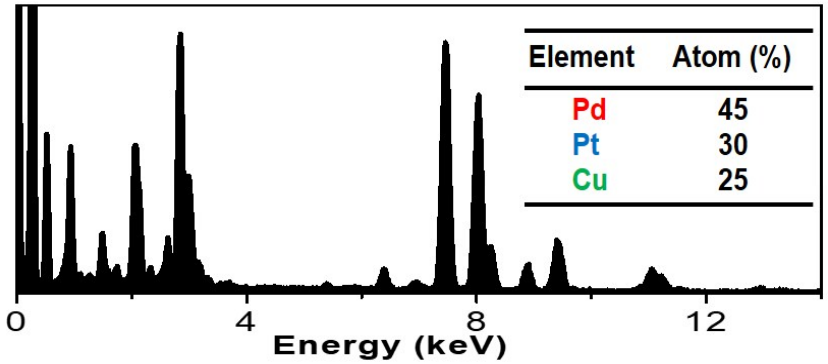

Figure S2. STEM-EDS spectra of trimetallic PdPtCu MHS@N-G in Figure 1, indicating the composition ratio of Pd/Pt/Cu is 45:30:25.

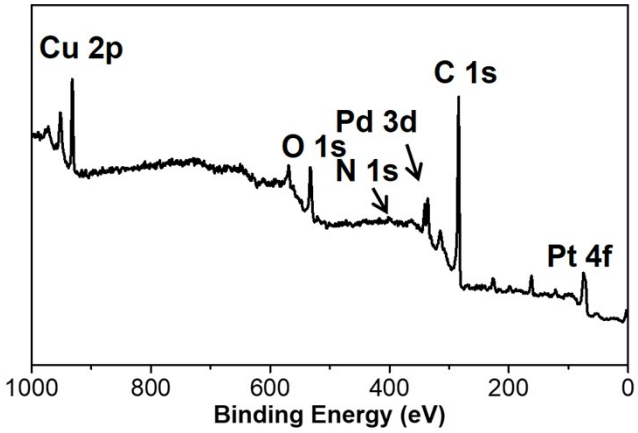

Figure S3. XPS survey spectrum of trimetallic PdPtCu MHS@N-G in Figure 1.

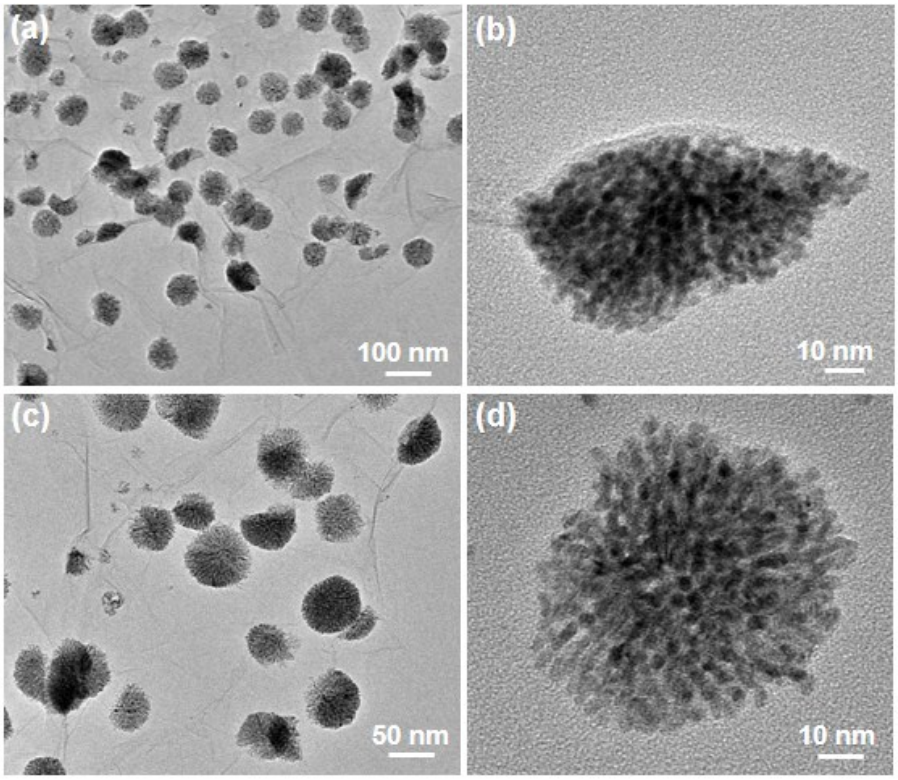

Figure S4. TEM images of PdPtCu MHS@N-G synthesized with the surfactant of (a, b) dihexadecyldimethylammonium chloride and (c, d) dimethyldistearylammonium chloride.

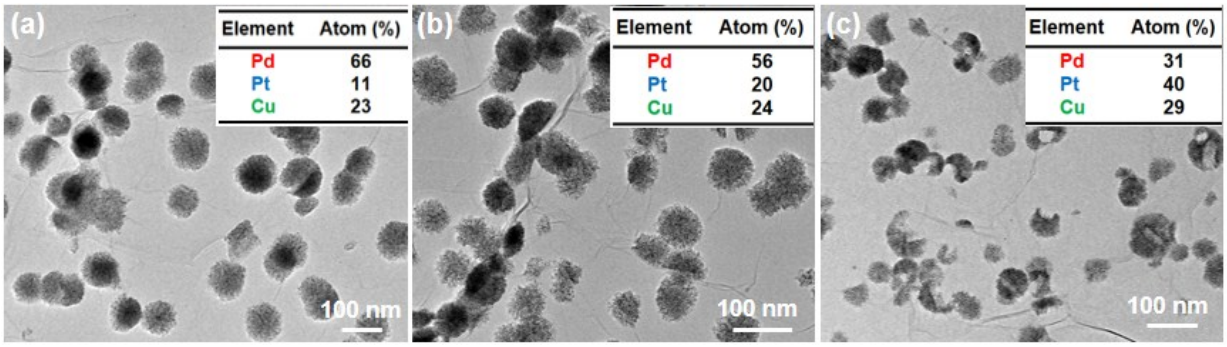

Figure S5. TEM images and corresponding elemental compositions of trimetallic PdPtCu MHS@N-G with different commotional ratios. MHS structure was slightly destroyed in the higher Pt content, possibly because of the different reduction potentials of H_2PdCl_4 and H_2PtCl_6.

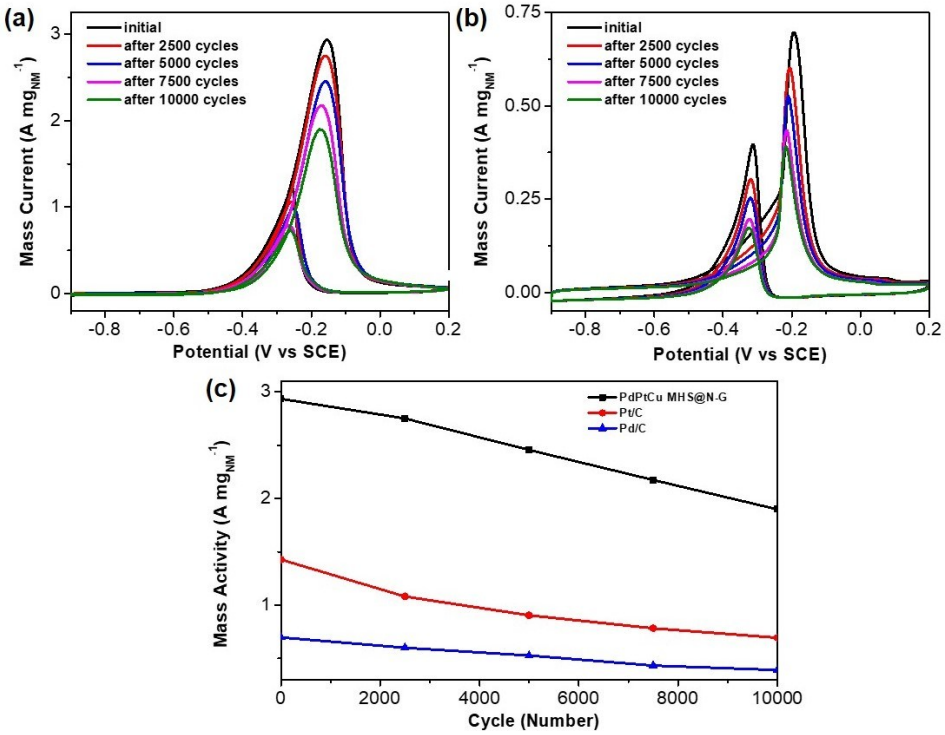

Figure S6. Cycling stabilities of (a) asymmetric PdPtCu MHS@N-G and (b) commercial Pd/C. (c) Summarized mass activities of asymmetric PdPtCu MHS@N-G and commercial Pd/C for MOR electrocatalysis of 10000 cycles.

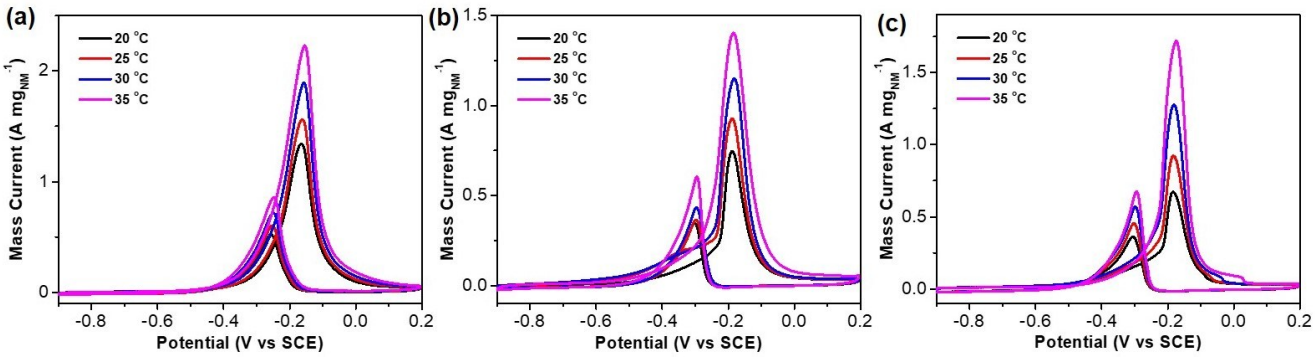

Figure S7. CV curves of (a) PdPt MHS@N-G, (b) Pd MHS@N-G, and (c) Pd/C collected in 1.0 M KOH and 1.0 M methanol under different test temperatures.

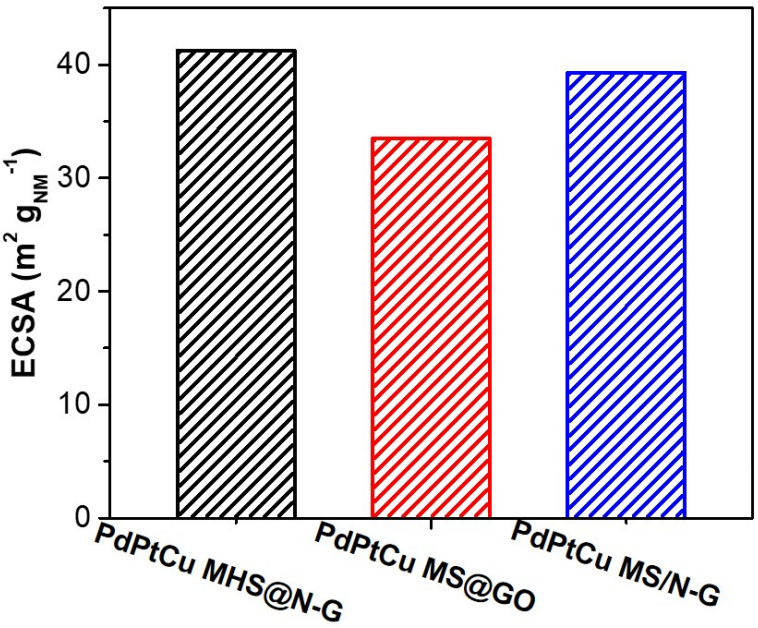

Figure S8. ECSA values of asymmetric PdPtCu MHS@N-G, PdPtCu MS@GO, and PdPtCu MS/N-G collected from CV curves in Figure 7a.

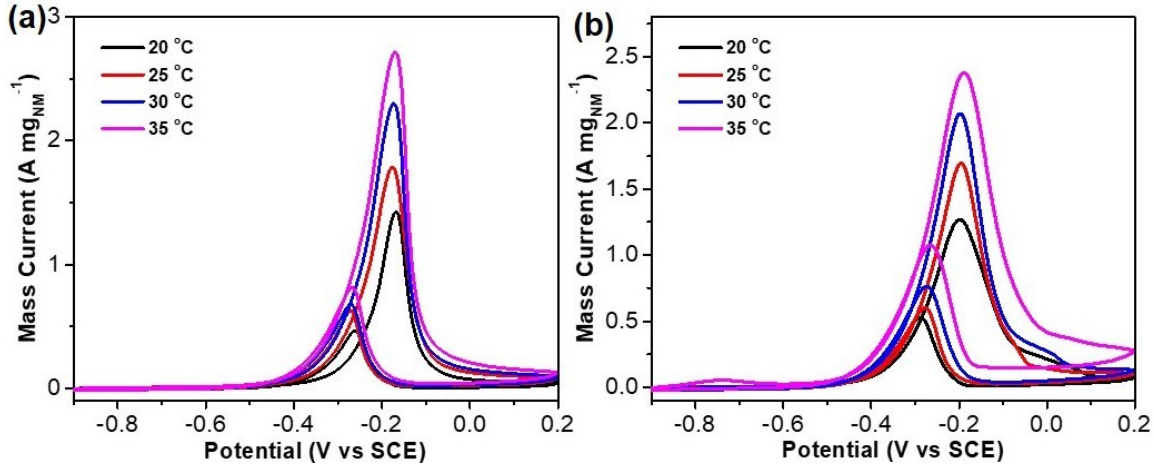

Figure S9. CV curves of (a) PdPtCu MS@GO and PdPtCu MS/N-G collected in 1.0 M KOH and 1.0 M methanol under different test temperatures.

Table 1. Summarizations of the activities of Pd-based nanocatalysts in MOR electrocatalysis.

Nanocatalysts	Measurement Conditions		Mass Activity ($A\ mg_{NM}^{-1}$)	References
	CH_3OH con. (M)	KOH con. (M)		
PdPtCu MHS@N-G	**1.0**	**1.0**	**3.01**	**This work**
PdPtCu Nanosheets	1.0	1.0	2.67	*Green Chem.* **2019**, *21*, 2367
PdCuRu Nanosheets	1.0	1.0	1.66	*ACS Appl. Mater. Interfaces* ***2019****, 11, 45, 42123*
PtRu/rGO	1.0	1.0	0.739	*J. Colloid Interface Sci.* ***2019****, 557, 729*
Pd/N-P-G	1.0	1.0	1.597	*J. Alloys Compd.* ***2019****, 785, 781*
Pd@PtNi	1.0	1.0	1.614	*ACS Appl. Nano Mater.* ***2018***, *1*, 3226
PtNi/C	1.0	1.0	1.75	*Nano Res.* ***2018****, 11, 2058*
Pd/SiO_2@rGO	1.0	1.0	1.533	*Appl. Surf. Sci.* ***2018****, 452, 11*
PdRuP	1.0	1.0	1.26	*Int. J. Hydrogen Energy* **2017**, *42*, 11229
PtPdBi nanoparticles	1.0	1.0	2.133	*Catalysts* **2017**, *7*, 208
$Pt_{50}Pd_{50}$	1.0	1.0	0.336	*Chem. Commun.* **2016**, *52*, 12737
$Pt/Ni(OH)_2$/rGO	1.0	1.0	1.07	*Nat. Commun.* **2015**, *6*, 10035
PtAu/PDA-RGO	1.0	1.0	0.645	*Electrochim. Acta* **2015**, *153*, 175
Pd/ZnO/GNs	1.0	1.0	0.818	*Langmuir* **2015**, *31*, 2576
PdCu /RGO	1.0	1.0	1.153	*J. Power Sources* **2015**, *228*, 160
PdCu/VrGO	1.0	1.0	0.763	*J. Power Sources* **2015**, *278*, 725
$Pt/RGO/TiO_2$/CF	1.0	1.0	0.364	*J. Solid State Electrochem.* **2014**, *18*, 515
PdAu/C	1.0	1.0	0.951	*J. Mater. Chem. A* **2013**, *1*, 9157
PdAu/RGO	1.0	1.0	1.218	*J. Mater. Chem. A* ***2013****, 1, 6579*
PtAuRu/RGO/GC	1.0	1.0	1.606	*J. Mater. Chem. A* **2013**, *1*, 7255
Pd/PTCDIIL/GO	1.0	1.0	0.616	*Electrochim. Acta* **2013**, *109*, 276
N-Pt/RGO/CF	1.0	1.0	1.073	*Int. J. Hydrogen Energy* **2013**, *38*, 6368